Supporting Information

Switching the memory behavior from binary to ternary by triggering the S_6^{2-} relaxation in polysulfide-bearing Zinc-organic complex molecular memories

Pan-Ke Zhou,[a+] Xiao-Li Lin,[a+] Mun Yin Chee,[b] Wen Siang Lew,[b] Tao Zeng,[c] Hao-Hong Li,*[a] Xiong Chen,*[a] Zhi-Rong Chen,[a] and Hui-Dong Zheng*[d]

[a] P. K. Zhou, X. L. Lin, Prof. H. H. Li, Prof. X. Chen, Prof. Z. R. Chen

Fujian Provincial Key Laboratory of Advanced Inorganic Oxygenated Materials, State Key Laboratory of Photocatalysis on Energy and Environment, College of Chemistry, Fuzhou University, Fujian 350108, China, E-mail: lihh@fzu.edu.cn (H. H. Li), chenxiong987@fzu.edu.cn (X. C), and zrchen@fzu.edu.cn (Z. R. Chen)

[b]M. Y. Chee, Prof. W. S. Lew, School of Physical and Mathematical Sciences, Nanyang Technological University, Singapore 637371, Singapore

[c]Dr. Tao. Z, Department of Materials Science and Engineering, National University of Singapore, Singapore 117575, Singapore

[d]Prof. H. D. Zheng, Fujian Engineering Research Center of Advanced Manufacturing Technology for Fine Chemicals, College of Chemical Engineering, Fuzhou University, Fuzhou, Fujian, 350108, China. E-mail: youngman@fzu.edu.cn (H. D. Zheng)

[+] These authors contributed equally to this work.

Experimental section

Materials and Physical Measurements. Pyridine, 3-methyl-pyridine, 2,2'-Bipyridine, 1,10-phenanthroline and zinc powder were provided by Aladdin (Shanghai, China). Other reagents and solvents (AR grade) were commercially available from Sinopharm Chemical Reagent without further purification. Fourier transform infrared (FT-IR) spectra were recorded on a Perkin-Elmer Spectrum-2000 FTIR spectrophotometer (4000-400 cm^{-1}) by dispersing the sample spread in KBr pellet. The UV-visible absorption spectra were recorded on a UV-2600 UV-Vis spectrophotometer (Shimadzu) in the wave range of 200-800 nm at room temperature. Powder X-ray diffraction (PXRD) measurements were done on a Philips X'Pert-MPD diffractometer equipped with Cu Kα radiation (1.54056 Å). The thermal stabilities were determined by TGA on a Mettler Toledo TGA/DSC3+ instrument heated from 30 to 800 °C at a rate 10 °C/min under a nitrogen atmosphere. Cyclic voltammetry (CV) was performed with a CHI660D Electrochemical Workstation (Shanghai Chenhua Instruments) by using of a conventional three-electrode cell. The HR-SEM images were taken on a Verios G4 field-emission scanning electron microscope. The AFM image was obtained with a ScanAsyst mode on a Bruker Dimension ICON (probe: ScanAsyst-AIR). The current-voltage (*I-V*) characteristics of FTO/active layer/Ag devices were measured using a KEYSIGHT B2911A source meter. The AFM measurements were executed on a Bruker Dimension ICON (probe:ScanAsyst-AIR) with a ScanAsyst mode, and KPFM surface potential distributions were obtained by using a SCM-PIT probe in AFM.

Synthesis

Synthesis of $ZnS_6(Py)_2$ (1): The synthesis process of four Zn/polysulfide/organic complexes is summarized in Scheme S1. Sulfur powder (3.52 g, 110 mmol) was added into 50 mL pyridine solvent at room temperature, and the mixture was stirred for 0.5 h. Afterwards, zinc powder (1.2 g, 18 mmol) was added into the above solution. The resultant mixture was refluxed at 90 °C under stirring condition for 3 h. Finally, after cooling to room temperature, the solution was filtered with the filtrate being kept at room temperature for 24 h to yield yellow crystals (1.5 g, 3.60 mmol, yield: 20 %). IR (KBr, cm^{-1}): 3050(w), 1600(s), 1480(s), 1450(s), 1210(s), 1070(s), 753(s), 698(s), 492(m), 324(m), 285(w), 201(w).

Synthesis of $ZnS_6(Mpy)_2$ (2): The synthesis of **2** was similar to that of **1**, except that 3-methyl-

pyridine (50 mL, 516 mmol) was used as starting material. The products were yellow crystals (1.3g, 2.92 mmol, yield: 16 %). IR (KBr, cm^{-1}): 3062(w), 1606(s), 1579(s), 1482(s), 1450(s), 1415(s), 1194(s), 1128(s), 1107(s), 1058(s), 796(s), 716(s), 494(m), 320(m), 289(w), 208(w).

Synthesis of ZnS_6(Bipy) (3): Sulfur powder (0.5 g, 15.6 mmol), 2,2'-bipyridine (0.26 g, 1.7 mmol) and zinc powder (0.6g, 9.2 mmol) were mixed in 25 mL DMF. The mixture was refluxed at a115 ℃ under stirring condition for 3h. After cooling to room temperature, the solution was filtered and the filtrate was kept at room temperature for 24 h to obtain yellow crystals (0.3g, 0.72 mmol, yield: 8 %). IR (KBr, cm^{-1}): 3050(w), 1660(s), 1600(s), 1480(s), 1440(s), 1090(s), 773(s), 733(s), 491(m), 324(m), 278(w), 189(w).

Synthesis of ZnS_6(Phen) (4): The synthesis details of **4** were similar to that of **3** except that 1,10-phenathtroline (0.6 g, 9.2 mmol) was used instead of 2,2'-bipyridine. Yellow crystals (0.4g, 0.91 mmol) with yield of 10 % could be obtained. IR (KBr, cm^{-1}): 3050(w), 1620(s), 1580(s), 1520(s), 1430(s), 850(s), 728(s), 486(m), 324(m), 285(w), 204(w).

Fabrications of memory devices The memory device with structure of FTO/Zn complex/Ag were fabricated by the following process. Firstly, the fluorine-doped tin oxide-coated glasses (FTO, 20×20 mm) were pre-cleaned using acetone, ethanol and water by ultrasonic spray for three times, and dried under vacuum. Secondly, as-prepared Zn-polysulfide-organic complexes were dissolved in DMF with concentrations of 2 mg/mL, which were spin-coated on the clean FTO substrates (speed: 200rpm for 10s firstly, and then 3000rpm for 10s). The films were further annealed at 60 ˚C for 6 h. Finally, Ag pastes were deposited as the top electrodes through a shadow mask with circular holes with a diameter of about 0.1-0.2 cm. The devices were dried at 60 ˚C for 1 h to improve their adhesive force.

X-ray single crystal diffraction Diffraction intensity data of Zn-polysulfide-organic complexes were obtained on a Bruker APEX II CCD area diffractometer equipped with a fine focus, 2.0 kW sealed tube X-ray source (Mo Kα radiation, λ = 0.71073 Å) operating at 293(2) K. Crystal structures were solved by the direct method with program SHELXS and refined with the least-squares program SHELXL.[1] The structures were verified using the ADDSYM algorithm from the program PLATON.[2] The refinement details are summarized in Table S1, selected bond lengths and angles are listed in Table S2, hydrogen bonds details and π-π interaction details at are given in Table S3 and S4. [CCDC: 2232734 (**1**), 2232735 (**2**), 2232736

(**3**) and 2232737 (**4**), contains the supplementary crystallographic data for this paper. This data can be obtained free of charge from The Cambridge Crystallographic Data Centre via www.ccdc.cam.ac.uk/data_request/cif.]

Table S1. Summary of the crystal data and structural determinations

	1	**2**	**3**	**4**
Empirical formula	$C_{10}H_{10}N_2S_6Zn$	$C_{12}H_{14}N_2S_6Zn$	$C_{10}H_8N_2S_6Zn$	$C_{12}H_8N_2S_6Zn$
Formula mass	415.95	444.00	413.93	437.95
Crystal system	Monoclinic	Triclinic	Monoclinic	Triclinic
Space group	*C2/c*	*P-1*	*C2/c*	*P-1*
a[Å]	13.6639(13)	9.1750(13)	18.958(4)	8.1617(9)
b[Å]	9.0204(8)	9.797(2)	7.3171(17)	9.4765(10)
c [Å]	14.8989(19)	11.3263(17)	22.257(5)	12.0105(15)
α[°]	90	83.744(7)	90	109.535(4)
β[°]	115.024(3)	75.751(5)	101.810(7)	99.066(4)
γ[°]	90	62.164(4)	90	100.714(4)
V[Å]	1664.0(3)	872.6(3)	3022.1(12)	835.64(17)
Z	4	2	8	2
D_c[g/cm3]	1.660	1.690	1.820	1.740
μ[mm^{-1}]	2.215	2.117	2.438	2.210
F(000)	840.0	452.0	1664.0	440.0
Reflections, total	8104	21908	19242	21633
Reflections, unique	1461[R_{int} = 0.0537]	3108[R_{int} =0.0523]	2724[R_{int} =0.1335]	2953[R_{int} =0.0450]
Reflections, observed	994	2949	1656	2195
Goodness-of-fit on *F*2	1.004	1.029	1.009	1.064
No. of parameters refined	88	193	172	190
R_1[$I>2\sigma(I)$]	0.0315	0.0549	0.0525	0.0667
wR_2[$I>2\sigma(I)$]	0.0647	0.1285	0.1175	0.1863
Residual extremes(e/$Å^3$)	0.262/-0.192	3.443/ -1.194	0.798/-0.450	1.729/ -0.763

Table S2. Selected bonds and angles of 1~4.

1					
Zn(1)-N(1)#1	2.069(2)	Zn(1)-N(1)	2.069(2)	Zn(1)-S(3)	2.2903(8)
Zn(1)-S(3)#1	2.2902(8)	S(1)-S(1)#1	2.072(2)	S(3)-S(2)	2.0516(12)
S(2)-S(1)	2.0389(13)	N(1)#1-Zn(1)-N(1)	103.06(12)	N(1)#1-Zn(1)-S(3)	107.48(7

N(1)-Zn(1)-S(3)	105.77(7)	N(1)#1-Zn(1)-S(3)#1	105.77(7)	N(1)-Zn(1)-S(3)#1	107.48(7)
S(3)-Zn(1)-S(3)#1	125.24(5)	S(2)-S(1)-S(1)#1	108.24(6)	S(1)-S(2)-S(3)	106.29(5)
Symmetry codes: #1 -x+1,y,-z+1/2					
2					
Zn(1)-N(1)	2.074(4)	Zn(1)-N(2)	2.066(4)	Zn(1)-S(1)	2.3093(14)
Zn(1)-S(6)	2.2889(14)	S(1)-S(2)	2.062(2)	S(3)-S(2)	2.078(2)
S(4)-S(3)	2.079(2)	S(5)-S(4)	2.049(2)	S(6)-S(5)	2.0523(18)
N(2)-Zn(1)-N(1)	108.10(16)	N(2)-Zn(1)-S(6)	107.58(12)	N(1)-Zn(1)-S(6)	103.76(12)
N(2)-Zn(1)-S(1)	104.96(12)	N(1)-Zn(1)-S(1)	108.10(12)	S(6)-Zn(1)-S(1)	123.65(5)
S(4)-S(5)-S(6)	107.31(9)	S(5)-S(4)-S(3)	108.27(9)	S(2)-S(3)-S(4)	106.23(10)
S(1)-S(2)-S(3)	108.75(9)				
3					
Zn(1)-N(1)	2.073(5)	Zn(1)-N(2)	2.076(5)	Zn(1)-S(1)	2.2682(18)
Zn(1)-S(6)	2.2859(18)	S(1)-S(2)	2.066(3)	S(3)-S(2)	2.044(2)
S(3)-S(4)	2.062(3)	S(5)-S(4)	2.029(2)	S(6)-S(5)	2.061(2)
N(1)-Zn(1)-N(2)	79.27(19)	N(1)-Zn(1)-S(1)	112.24(14)	N(2)-Zn(1)-S(1)	115.61(14)
N(1)-Zn(1)-S(6)	107.75(13)	N(2)-Zn(1)-S(6)	107.50(14)	S(1)-Zn(1)-S(6)	125.03(7)
S(4)-S(5)-S(6)	107.03(10)	S(2)-S(3)-S(4)	107.80(11)	S(5)-S(4)-S(3)	107.40(10)
S(3)-S(2)-S(1)	107.75(11)				
4					
Zn(1)-N(1)	2.089(6)	Zn(1)-N(2)	2.083(6)	Zn(1)-S(1)	2.262(3)
Zn(1)-S(6)	2.281(2)	S(1)-S(2)	2.019(4)	S(2)-S(3)	2.058(4)
S(4)-S(3)	2.075(4)	S(5)-S(4)	2.062(5)	S(6)-S(5)	2.062(4)
N(2)-Zn(1)-N(1)	80.3(2)	N(2)-Zn(1)-S(1)	115.49(18)	N(1)-Zn(1)-S(1)	107.11(16)
N(2)-Zn(1)-S(6)	107.85(17)	N(1)-Zn(1)-S(6)	115.28(16)	S(1)-Zn(1)-S(6)	123.02(10)
S(4)-S(5)-S(6)	107.46(14)	S(5)-S(4)-S(3)	109.51(19)	S(1)-S(2)-S(3)	107.8(2)
S(2)-S(3)-S(4)	106.36(19)				

Table S3. Hydrogen bridging details of this work.

Compound	D–H···A	D–H/Å	H···A/Å	D···A/Å	∠(D–H···A)/°	Symmetry codes
2	C(12)-H(12)···S(1)	0.93	2.86	3.496(6)	126	
3	C(4)-H(4)···S(6)	0.93	2.87	3.738(7)	155	1-x,1-y,1-z
	C(8)-H(8)···S(3)	0.93	2.84	3.692(7)	153	x,1-y,1/2+z
4	C(12)-H(12)···S(1)	0.93	2.86	3.592(10)	137	1-x,1-y,1-z

Table S4. π–π stacking interactions in this work (lengths in Å and angles in °)

Complex	Cg(I)···Cg(J)	Symmetry code	Dist. Centroids	Dihedral angle	CgI_Perp dist.	CgJ_Perp dist.
3	Cg(1)→Cg(2)	1-x,1-y,1-z	3.715(4)	2.2(3)	3.447(2)	3.469(2)
	Ring C(1) : N(1)→C(1)→C(2)→C(3)→C(4)→C(5)→					
	Ring Cg(2) : N(2)→C(6)→C(7)→C(8)→C(9)→C(10)→					
	Cg(1)→Cg(2)	1-x,1-y,1-z	3.650(5)	1.0(3)	3.529(3)	3.526(3)

	Cg(2)→Cg(3)	1-x,1-y,1-z	3.638(4)	1.2(3)	3.525(3)	3.506(2)
	Cg(1)→Cg(4)	1-x,1-y,1-z	3.539(5)	0.6(3)	3.529(3)	3.529(2)
4	Cg(2)→Cg(5)	-x,1-y,1-z	3.534(4)	0.4(3)	3.477(2)	3.472(3)
	Ring Cg(1): N(1)→C(1)→C(2)→C(3)→C(4)→C(5)→					
	Ring Cg(2): C(4)→C(5)→C(6)→C(10) →C(11)→C(12) →					
	Ring Cg(3): N(1)→C(1)→C(2)→C(3)→C(4) →C(12) →C(11)→C(10) →C(9)→C(8)→C(7)→N(2) →C(6)→C(5) →					
	Ring Cg(4): N(1)→C(1)→C(2)→C(3)→C(4) →C(12) →C(11)→C(10)→C(6)→C(5) →					
	Ring Cg(5): N(2)→C(6)→C(5)→C(4)→C(12) →C(11) →C(10)→C(9)→C(8)→C(7) →					

Table S5. The C_V parameters of Zn-complex-based devices.

Devices	C_V, HRS (%)	C_V, LRS (%)	C_V, V_{th1}/V_{SET} (%)	C_V, V_{th2}/V_{RESET} (%)
FTO/**1**/Ag	0.32	0.26	0.20	0.07
FTO/**2**/Ag	0.15	0.14	0.12	0.18
FTO/**3**/Ag	0.24	0.32	0.18	0.36
FTO/**4**/Ag	0.20	0.17	0.18	0.12

Table S6. The important resistive switching parameters of zinc complex-based memorizers.

Devices	Switching level	V_{Set}/V_{Reset} or V_{th1}/V_{th2} (V)	I_{OFF}/A	I_{ON1}/A	I_{ON2}/A	ON2/ON1/OFF ratio	Ternary yield (%)
FTO/**1**/Ag	Binary RRAM	+0.41/-3.97	$10^{-4.31}$	$10^{-2.27}$	/	$10^{2.04}$	-
FTO/**2**/Ag	Binary RRAM	+0.81/-3.17	$10^{-4.02}$	$10^{-2.00}$	/	$10^{2.02}$	-
FTO/**3**/Ag	Ternary WORM	+0.58/+1.47	$10^{-6.16}$	$10^{-3.89}$	$10^{-1.94}$	$10^{4.22}/10^{2.27}/1$	74
FTO/**4**/Ag	Ternary WORM	+0.73/+1.29	$10^{-6.69}$	$10^{-4.11}$	$10^{-1.84}$	$10^{4.85}/10^{2.58}/1$	78

Table S7. The memory parameters of WORM ternary devices and this work.

Devices	V_{th1}/V_{th2} (V)	ON2/ON1/OFF ratio	Ternary yield(%)	Ref.
ITO/Azo/Al	-1.37/-2.09	$10^{6.0}/10^{2.0}/1$	/	[S3]
ITO/OZA-SO/Al	-0.80/-3.50	$10^{6.20}/10^{3.38}/1$	/	[S4]
ITO/ Spiro-OMeTAD/ Al	+2.10/+4.00	$10^{7}/10^{4}/1$	86	[S5]
FTO/M-C/Ag	+1.14/+1.70	$10^{4.6}/10^{3.1}/1$	74	[S6]
FTO/PTPT@PS/Ag	+1.05/+1.72	$10^{6.44}$:$10^{4.47}$:1	50	[S7]
ITO/P-NCz-Na-PEG/Al	-1.10/-4.50	$10^{3.0}$:$10^{1.0}$:1	40	[S8]
ITO/ NI_2TDPP/Au	-1.31/-2.25	$10^{8.0}$:$10^{4.0}$:1	70	[S9]
ITO/Ti_3C_2Tx-OP MXene/Al	-2.10/-3.70	$10^{6.8}$:$10^{2.7}$:1	58	[S10]
ITO/Rh B/Al	+2.52/+3.18	$10^{6.0}$:$10^{4.0}$:6	52	[S11]
ITO/NACB/Al	-1.79/-2.88	$10^{4.0}$:$10^{2.0}$:1	/	[S12]
ITO /Polydopamine film/Al	+1.50/+3.50	$10^{9.0}$:$10^{6.0}$:1	45	[S13]

ITO / ^{t}Bu-TEBT /Al	+1.40/+2.60	$10^{5.0}$:$10^{3.0}$:1	66	[S14]
ITO/**4**/Ag	+0.73/+1.29	$10^{4.85}$/$10^{2.58}$/1	78	This work

Scheme S1. The synthetic process of Zn/polysulfide/organic complexes.

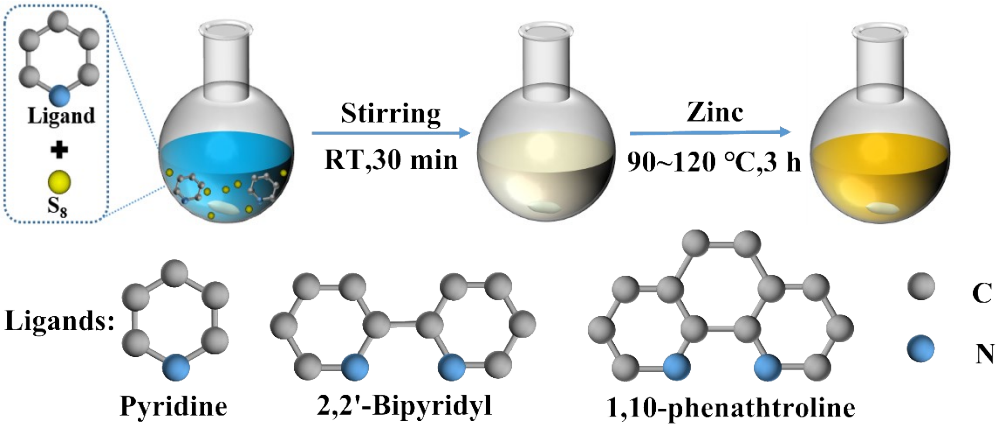

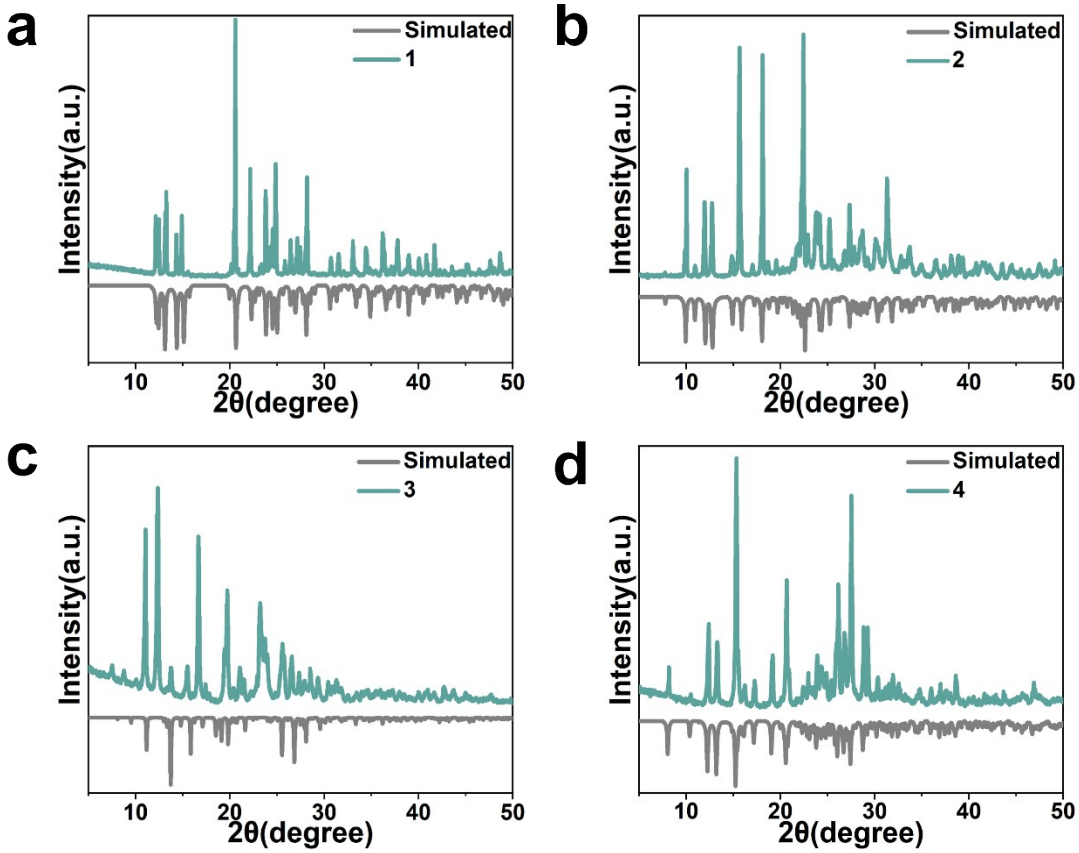

Fig. S1. PXRD patterns of the Zn/polysulfide/organic complexes: (a) **1**; (b) **2**; (c)**3**; (d) **4**.

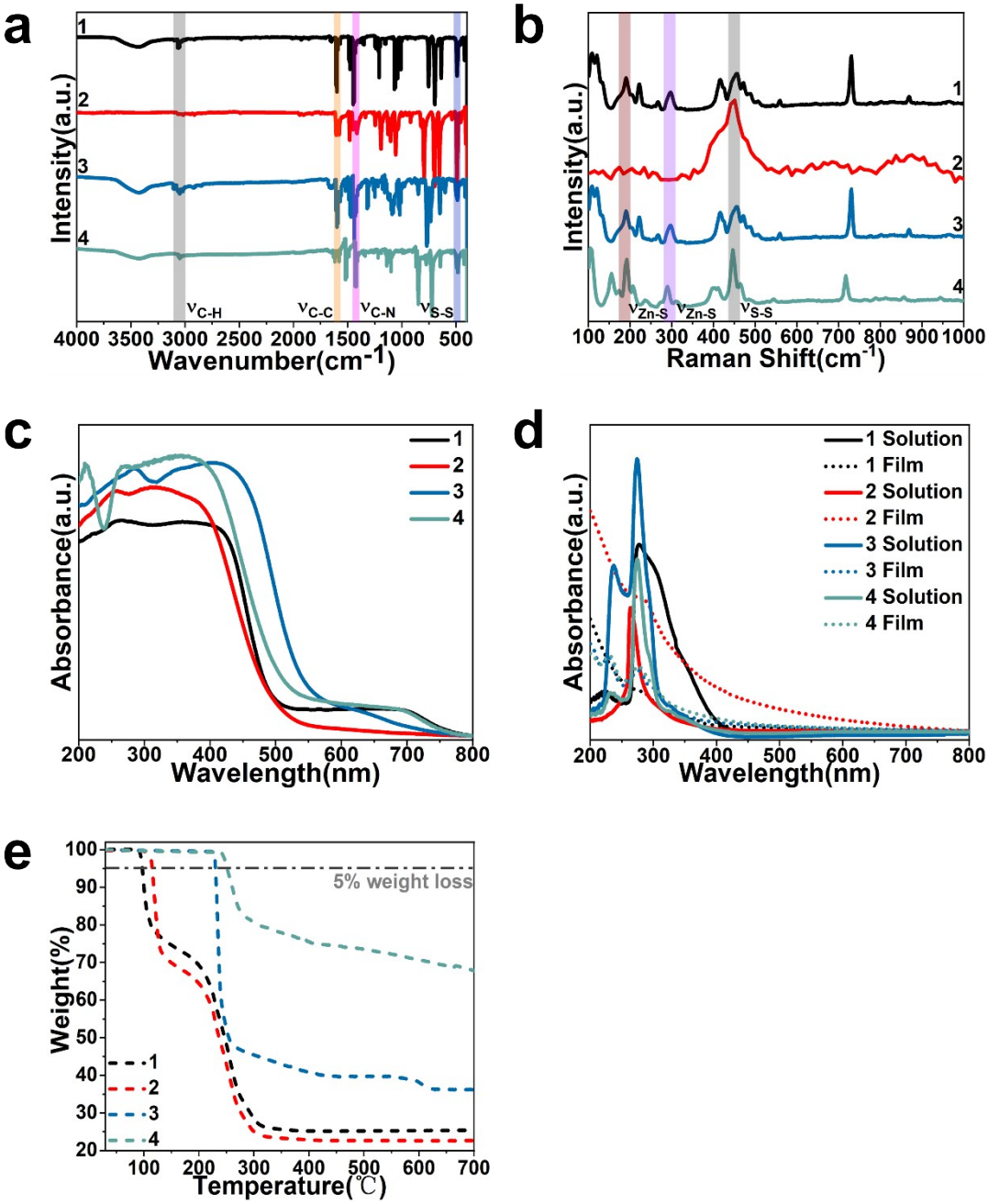

Fig. S2. Spectra characterizations of Zn/polysulfide/organic complexes: (a) FT-IR; (b) Raman; (c) solid state adsorption spectra; (d) UV-vis in DMF and on FTO films; (e) TGA curves.

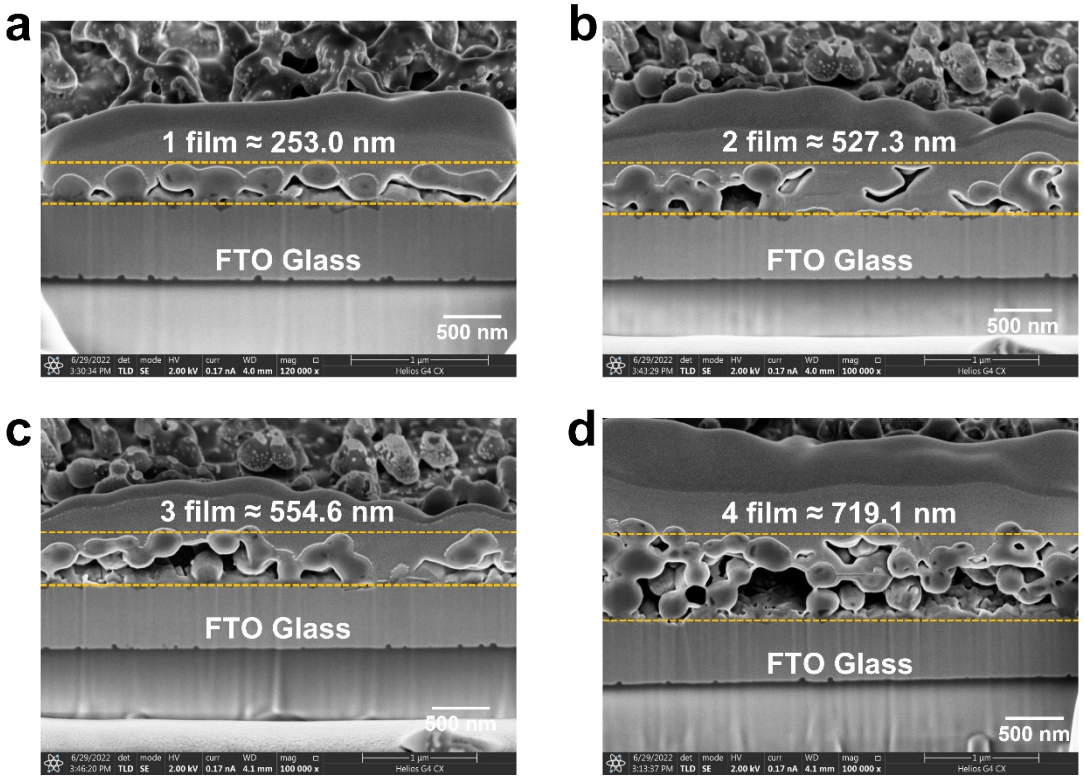

Fig. S3. Cross-sectional images of memory devices:(a) FTO/**1**/Ag; (b) FTO/**2**/Ag; (c) FTO/**3**/Ag; (d) FTO/**4**/Ag.

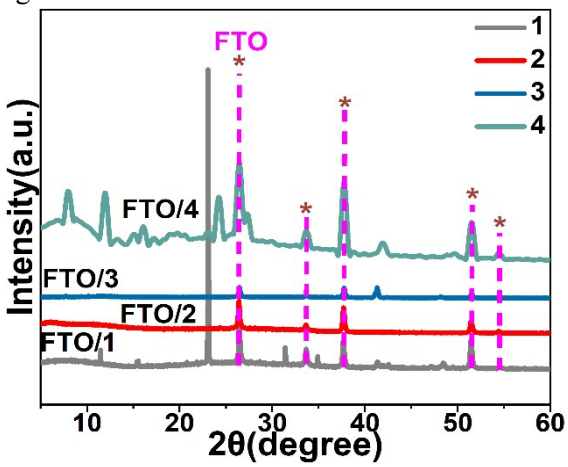

Fig. S4. XRD patterns of Zn-complex powders and FTO/Zn-complex films.

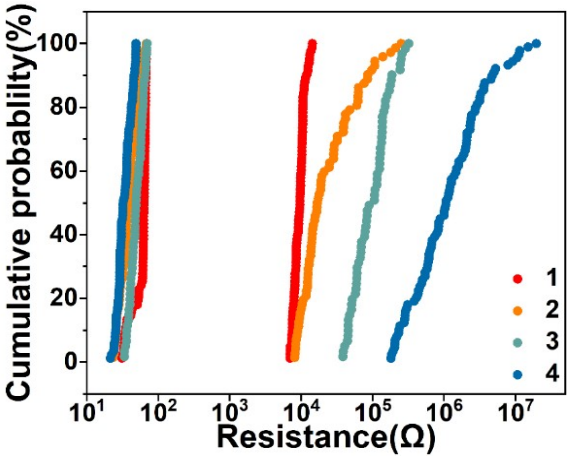

Fig. S5. The cumulative probability (CP) of the distribution of the HRS and LRS values for the FTO/Zn-complex/Ag memory devices.

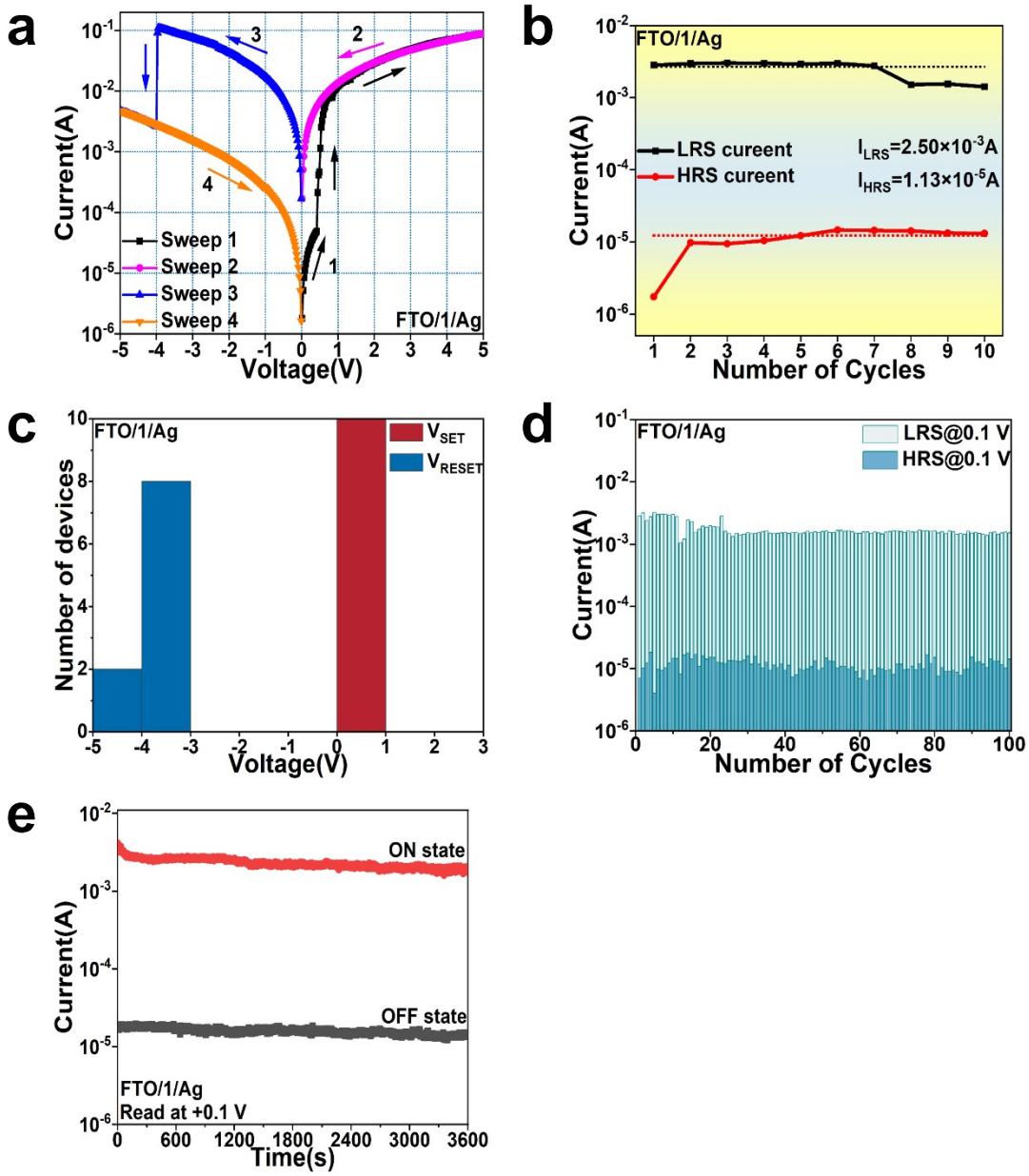

Fig. S6. Bipolar binary nonvolatile memory performance of FTO/**1**/Ag: (a) *I-V* curves showing four scanning ranges; (b) the averaged HRS and LRS currents calculated from 10 cycles; (c) the averaged V_{Set}/V_{Reset} calculated from 10 cycles; (d) cycle endurance showing 100 cycles; (e) retention stability of FTO/**1**/Ag device at "OFF" and "ON" states under a constant "read" voltage of +0.1 V.

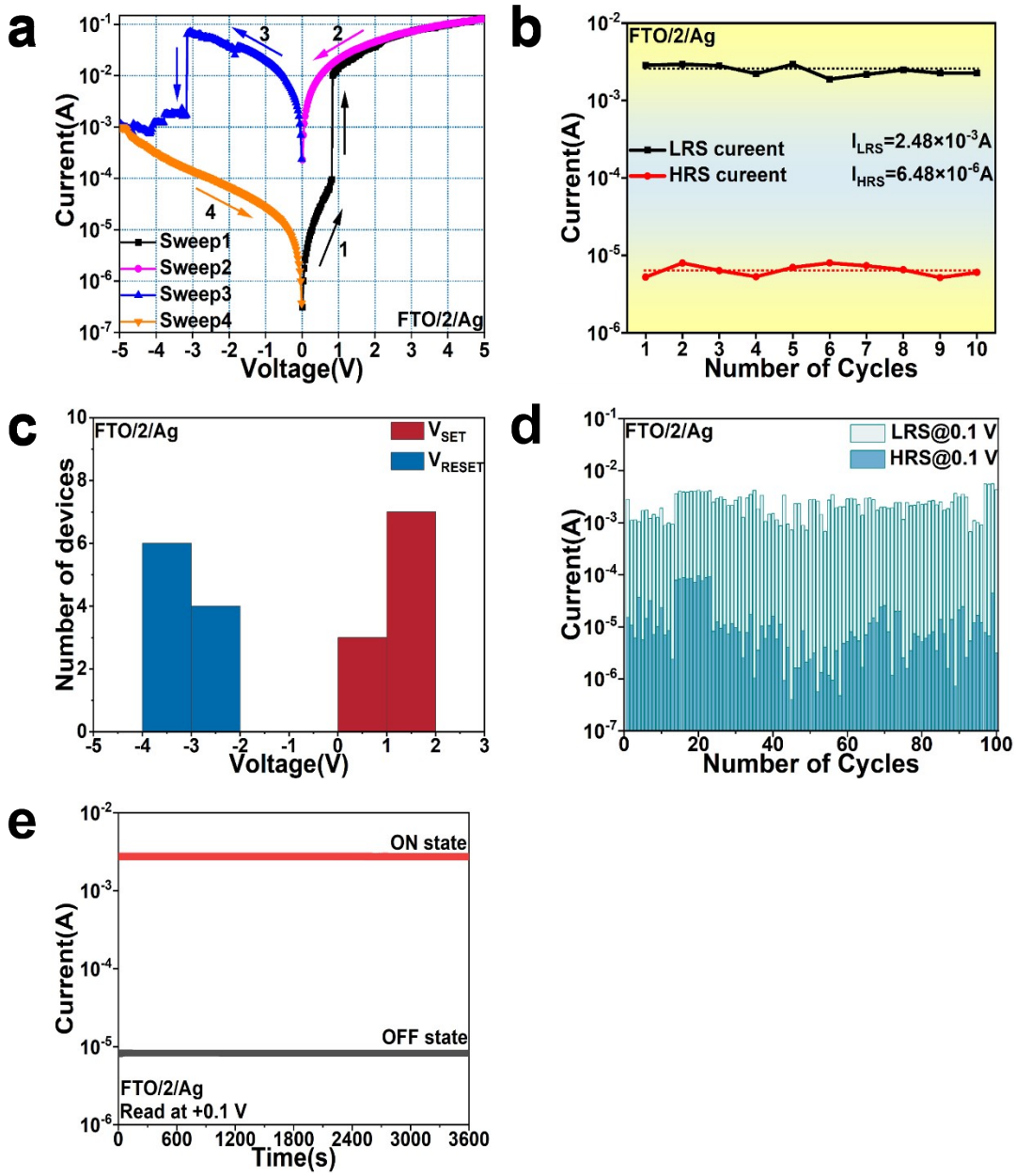

Fig. S7. Bipolar binary nonvolatile memory performance of FTO/**2**/Ag: (a) *I-V* curves showing four scanning ranges; (b) the averaged HRS and LRS currents calculated from 10 cycles; (c) the averaged V_{Set}/V_{Reset} calculated from 10 cycles; (d) cycle endurance showing 100 cycles; (e) retention stability of FTO/**2**/Ag device at "OFF" and "ON" states under a constant "read" voltage of +0.1 V.

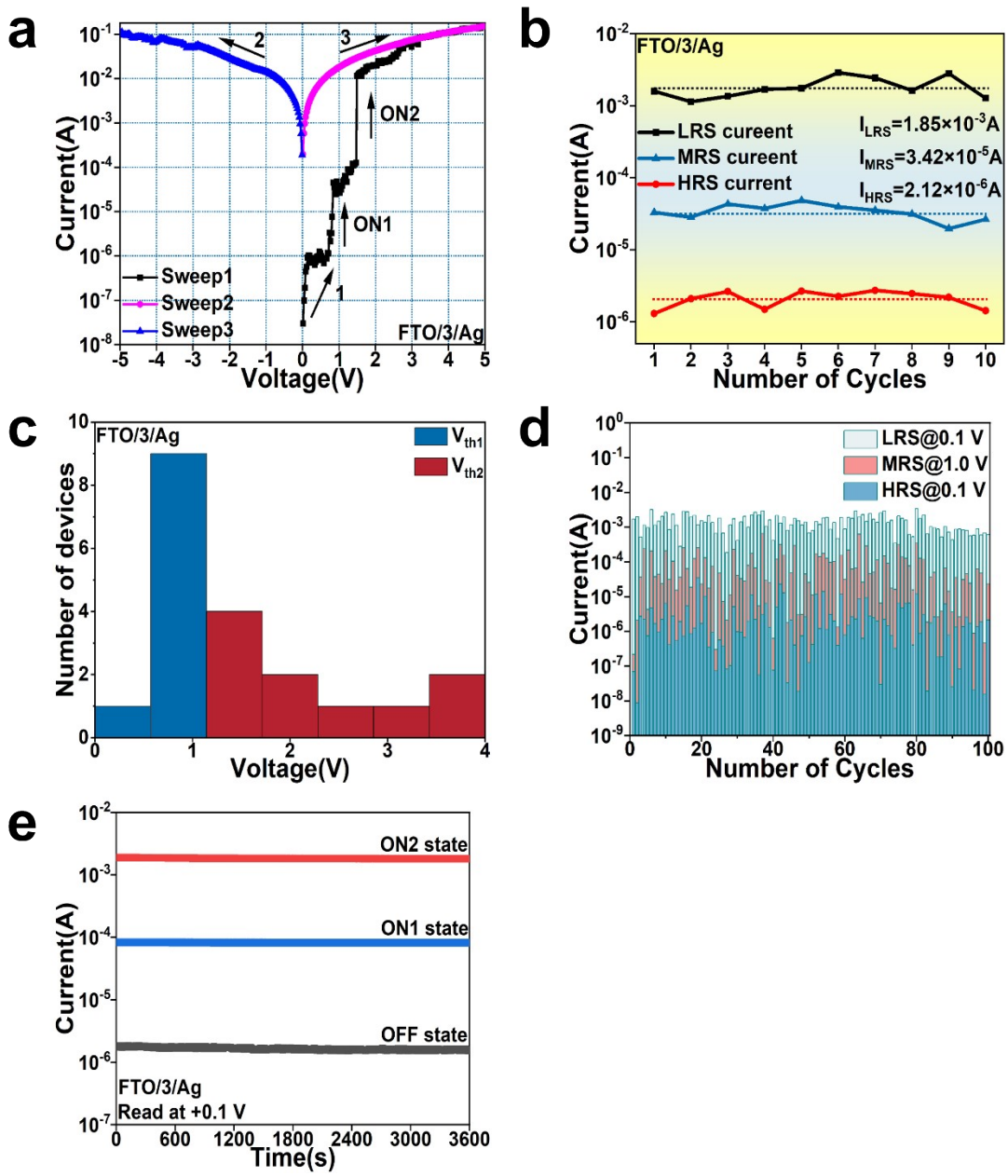

Fig. S8. (a) *I-V* characteristics showing the OFF-to-ON1 then to ON2 transitions of FTO/**3**/Ag device; (b) stabilities of the device in HRS, MRS, LRS states under constant stress (0.1 V for "OFF" state, 1.0 V for "ON1", and 0.1 V for "ON2" state); (c) distribution of the switching threshold voltages among 10 memory devices; (d) stability showing the HRS, MRS, LRS states currents with 100 cycles; (e) retention stability of FTO/**3**/Ag device at "OFF", "ON1", and "ON2" states under a constant "read" voltage of +0.1 V.

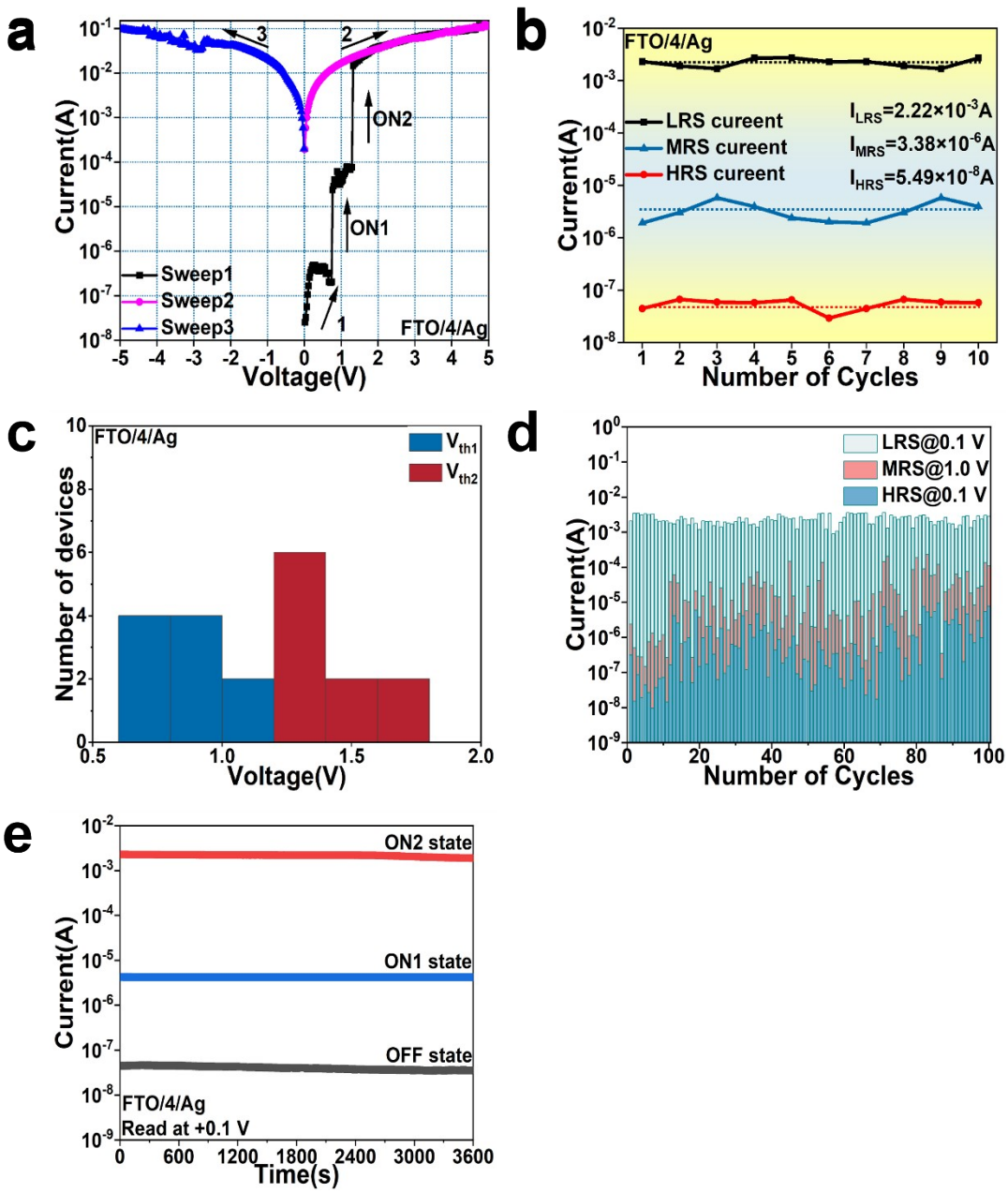

Fig. S9. (a) *I-V* characteristics showing the OFF-to-ON1 then to ON2 transitions of FTO/**4**/Ag device; (b) stabilities of the device in HRS, MRS, LRS states under constant stress (0.1 V for "OFF" state, 1.0 V for "ON1", and 1.0 V for "ON2" state). (b) distribution of the switching threshold voltages among 10 memory devices; (d) stability showing the HRS, MRS, LRS states currents with 100 cycles; (e) retention stability of FTO/**4**/Ag memory device at "OFF", "ON1", and "ON2" states under a constant "read" voltage of +0.1 V.

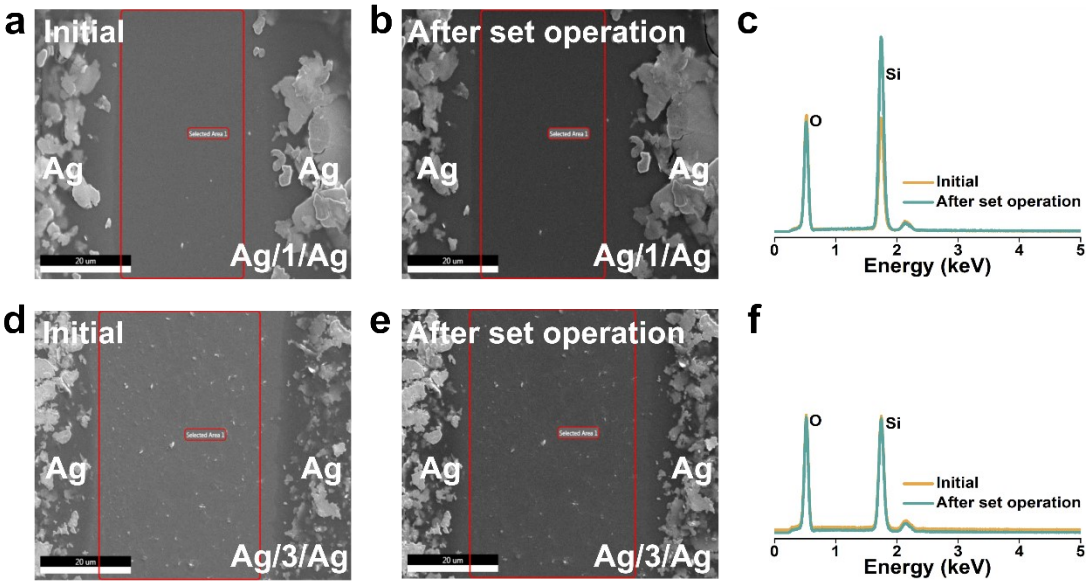

Fig. S10. (a, b) The SEM images of a planar Ag/**1**/Ag device before and after SET operation (compliance current: 0.5 A); (c) EDS spectra of a planar Ag/**1**/Ag device in same regions before and after SET operation; (d, e) The SEM images of a planar Ag/**3**/Ag device before and after SET operation (compliance current: 0.5 A); (f) EDS spectra of a planar Ag/**3**/Ag device in same regions before and after SET operation.

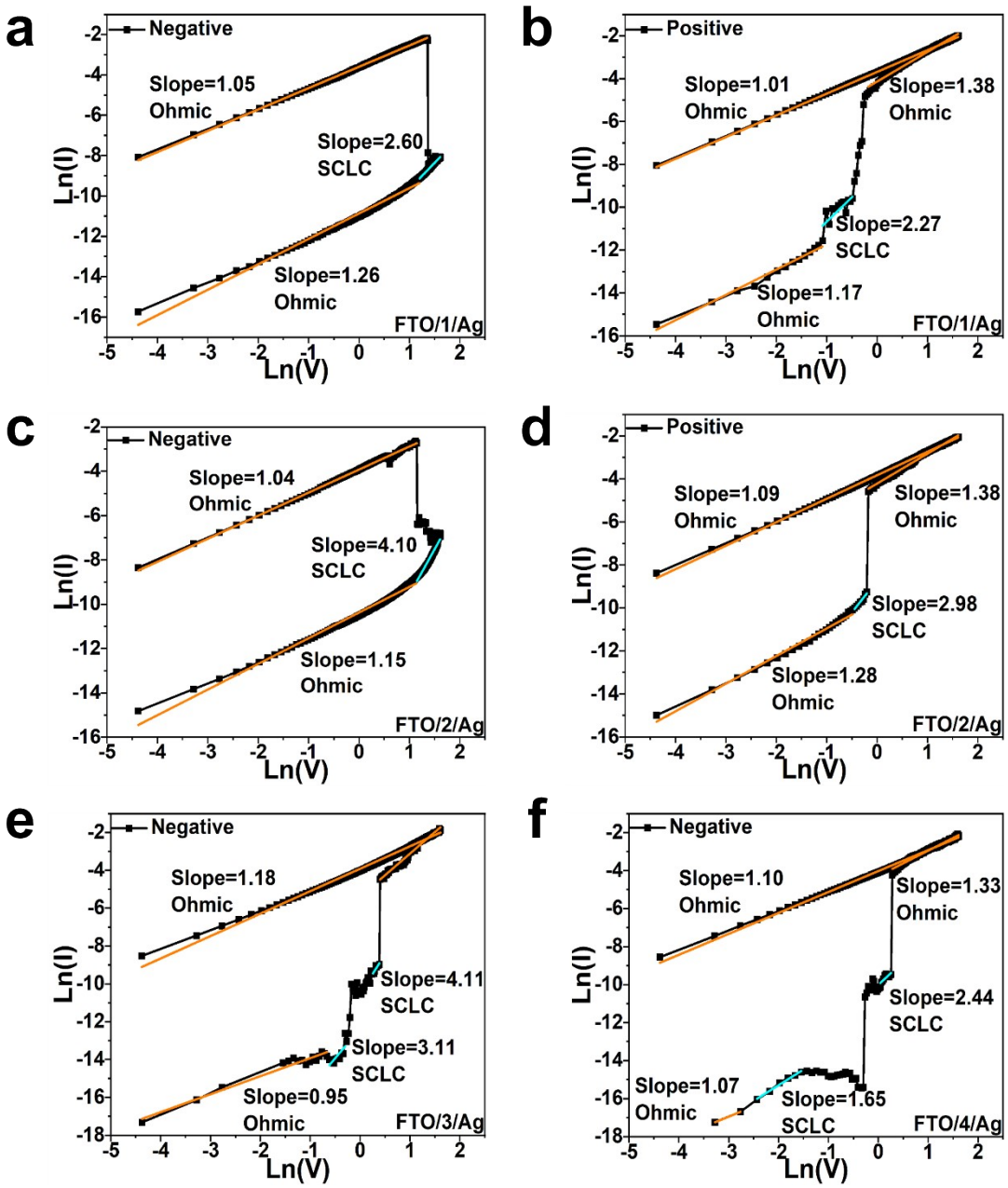

Fig. S11. Log-log plots on the *I-V* curves: (a) FTO/**1**/Ag under negative voltage sweep; (b) FTO/**1**/Ag under positive voltage sweep; (c) FTO/**2**/Ag under negative voltage sweep; (d) FTO/**2**/Ag under positive voltage sweep; (e) FTO/**3**/Ag under negative voltage sweep; (f) FTO/**4**/Ag under negative voltage sweep.

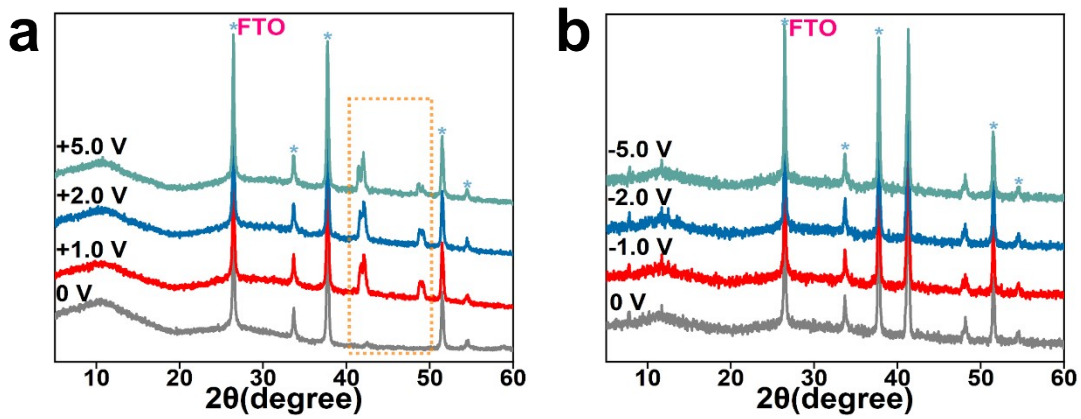

Fig. S12. Voltage-dependent XRD patterns: (a) FTO/**2** film: (b) FTO/**3** film.

References

[S1] G. Sheldrick, *Acta Crystallogr. A*, 2008, **64**, 112-122.

[S2] A. Spek, *J. Appl. Crystallogr.*, 2003, **36**, 7-13.

[S3] H. Li, Q. Xu, N. Li, R. Sun, J. Ge, J. Lu, H. Gu and F. Yan, *J. Am. Chem. Soc.*, 2010, **132**, 5542-5543.

[S4] Q. F. Gu, J. H. He, D. Y. Chen, H. L. Dong, Y. Y. Li, H. Li, Q. F. Xu and J. M. Lu, *Adv. Mater.*, 2015, **27**, 5968-5973.

[S5] Y. Y. Zhao, W. J. Sun, J. H. He and J. M. Lu, *Adv. Electron. Mater.*, 2019, **5**, 1800964.

[S6] K. Song, H. Yang, B. Chen, X. Lin, Y. Liu, Y. Liu, H. Li, S. Zheng and Z. Chen, *Appl. Surf. Sci.*, 2023, **608**, 155161.

[S7] Y. Z. Liu, Y. Liu, B. J. Chen, H. L. Yang, X. L. Lin, H. H. Li and Z. R. Chen, *Mater. Today Commun.*, 2022, **33**, 105026.

[S8] G. Wang, H. Li, Q. Zhang, C. Zhang, J. Yuan, Y. Wang and J. M. Lu, *Small*, 2022, **18**, 2202637.

[S9] Y. Li, C. Zhang, S. Ling, C. Ma, J. Zhang, Y. Jiang, R. Zhao, H. Li, J. Lu and Q. Zhang, *Small*, 2021, **17**, 2100102.

[S10] W. J. Sun, Y. Y. Zhao, X. F. Cheng, J. H. He, J. M. Lu, *ACS Appl. Mater. Interfaces*, 2020, **12**, 9865-9871.

[S11] J. Wang, X. F. Cheng, W. H. Qian, Y. Y. Zhao, J. H. He, Q. F. Xu, H. Li, D. Y. Chen, N. J. Li and J. M. Lu, *J. Mater. Chem. C.*, 2020, **8**, 7658-7662.

[S12] H. Cao, Q. Zhang, H. Li and J. M. Lu, *J. Mater. Chem. C.*, 2021, **9**, 569-574.

[S13] Y. Y. Zhao, X. F. Cheng, W. H. Qian, J. Zhou, W. J. Sun, X. Hou, J. H. He, H. Li, Q. F. Xu, N. J. Li, D. Y. Chen and J. M. Lu, *Chem. Asian. J.*, 2018, **13**, 1744-1750.

[S14] X. Cheng, H. Lian, L. Yao, W. Xia, J. Han, J. Fan, Q. Dong and W. Y. Wong, *Appl. Surf. Sci.*, 2022, **599**, 153877.